Supporting Information

Kawasaki and Ordway 10.1073/pnas.0907144106

SI Methods

Synaptic Electrophysiology. Flies were anesthetized using CO_2 and mounted in Tackiwax (Boekel Industries) essentially as described (1). Two-electrode voltage clamp was performed with a TEV-200 amplifier (Dagan Corporation) using recording (≈15 MΩ) and current passing (5–7 MΩ) microelectrodes filled with 3M KCl. The recording solution consisted of (in mM): 128 NaCl/2 KCl/4 $MgCl_2$/1.8 $CaCl_2$/5 Hepes/36 sucrose. The pH was adjusted to 7.0 using NaOH. Low calcium recording solution contained (in mM): 128 NaCl/2 KCl/5.6 $MgCl_2$/0.2 $CaCl_2$/5 Hepes/36 sucrose, pH 7.0. The recording chamber (5 mL) was perfused with recording solution at 1 mL/min. Temperature control was achieved using a TC-202A temperature controller and PDMI-2 microincubator (Harvard Apparatus). Temperature shifts from 20 to 33 °C required ≈3.5 min. Excitatory postsynaptic currents (EPSCs) were recorded at a holding potential of −20 mV, which optimized the recording conditions and did not alter any previously characterized dorsal longitudinal flight muscle (DLM) synaptic phenotypes. Before initiating EPSC recordings, the membrane potential was clamped to −20 mV for ≈10 min at 20 °C. Deviations from the command potential during recording of synaptic currents typically did not exceed 1 mV. For analysis of paired-pulse (PP) facilitation, each experiment represents the average of 2–5 consecutive PP trials (separated by a 20-s intertrial interval) from one preparation. Data were acquired using Pulse software (Heka Electronik) and an ITC-16 laboratory interface (Instrutech). Stimulation of DLM motor axons was achieved with a Master-8 Stimulator (A.M.P.I.). Synaptic currents were low-pass filtered at 5 kHz and acquired at 25 kHz. Measurements of synaptic current amplitudes were carried out in the Mini Analysis Program (Synaptosoft) and curve-fitting was performed using IGOR Pro (Wavemetrics). Excel (Microsoft Corp.) was used for analysis of numerical data, statistics, and graphing. All numerical data are reported as the mean ± SEM. Using an unpaired Student's t test, statistical significance was assigned to comparisons with $P \leq 0.05$.

Properties of *comatose* [*N*-Ethylmaleimide-Sensitive Factor (NSF)] and *SNAP-25^{TS}* Synaptic Phenotypes. Electrophysiological experiments were carried out at 20 or 33 °C. At 33 °C, for both the *comatose^{ST17}* and *SNAP-25^{TS}* mutants, similar synaptic phenotypes were observed in flies homozygous for the temperature sensitive (TS) mutation or carrying the mutation *in trans* to a deficiency (deletion) removing the gene. Although it is difficult to assess relative levels of protein activity at different temperatures, because of temperature-dependent changes in synaptic function (and neural activity in the case of *intact* flies), analogous activity-dependent synaptic phenotypes were observed at 36 °C in *comatose^{ST17}* (2) and *SNAP-25^{TS}*. Recording at the restrictive temperature of 33 °C provides sufficient stability for demanding studies of recovery from depression and facilitates direct comparison to other mutants not included in the present study. For comparison to earlier studies of *SNAP-25^{TS}* at larval neuromuscular synapses (3), recordings at 37 °C were also performed at adult neuromuscular synapses in this mutant. Consistent with previous work (3), these recordings indicated that the initial EPSC amplitude is reduced in *SNAP-25^{TS}* with respect to WT. However, the WT EPSC waveform was preserved under these conditions and further activity-dependent reduction in the EPSC amplitude resembled that observed at 33 or 36 °C. Whether or not the initial amplitude reduction reflects an effect of *SNAP-25^{TS}* on synaptic vesicle fusion at 37 °C was not addressed in our study. Together, our findings suggest that the *SNAP-25^{TS}* mutation preserves the well-established function of SNAP-25 in synaptic vesicle fusion under our typical recording conditions and selectively disrupts activity-dependent aspects of SNAP-25 function.

The temperature dependence of the *comatose* (NSF) and *SNAP-25^{TS}* synaptic phenotypes was examined at a permissive temperature of 20 °C (Fig. S1). Both mutants exhibited WT synaptic function in response to 1- and 5-Hz stimulation. The limits of the conditional nature of these phenotypes were examined by employing higher frequency stimulation at 20 °C. At 20 Hz (100 pulses), the level of depression in *SNAP-25^{TS}* closely resembled that of WT, whereas *comatose* (NSF) exhibited a modest enhancement (Fig. S1*C*). However, prolonged 20-Hz stimulation of *comatose* (NSF) synapses at 20 °C produced severe depression with respect to WT, resembling that observed at 33 °C under the same conditions (Fig. S4). The preceding observations indicate that the *comatose* (NSF) and *SNAP-25^{TS}* synaptic phenotypes are highly conditional, but that prolonged high-frequency stimulation may exceed the capacity of mutant NSF to catalyze sufficient disassembly of SNARE complexes to sustain WT neurotransmitter release.

Immunocytochemical Analysis. To observe the distribution of SYNTAXIN and SNAP-25 after synaptic stimulation, DLM preparations maintained at 33 °C were stimulated for 1 min at 20 Hz before fixation with 33 °C chemical fixative. Samples were fixed for an additional 30 min at room temperature and further processing was carried out as described previously. Imaging of CAC1-EGFP was performed by observation of native EGFP fluorescence. The primary and secondary antibodies used in this study are described below. Mounted DLM neuromuscular synapse preparations were imaged using an Olympus FV1000 confocal microscope with a PlanApo 60 × 1.4 numerical aperture oil objective (Olympus Optical) and z-step size of 0.2 μm. Images were acquired and processed with Fluoview software (Olympus Optical).

The following primary antibodies were used for immunocytochemistry. Rabbit anti-SNAP-25 (1:200) [kindly provided by David Deitcher (Cornell University, Ithaca, NY)]; mAb 8C3 anti-SYNTAXIN (1:20) (Developmental Studies Hybridoma Bank, University of Iowa); mAb nc82 anti-BRP (BRUCHPILOT) (1:50) [kindly provided by Erich Buchner (Universitaet Wuerzburg, Germany)] (4); rabbit anti-DPAK (*Drosophila* p21-activated kinase) (1:2,000) [kindly provided by Nicholas Harden (Simon Fraser University, Canada)] (5); and Cy5-conjugated rabbit anti-HRP (1:200) (Jackson Immunoresearch Laboratories). A rabbit polyclonal antiserum against the luminal (intravesicular) domain of n-SYB was generated essentially as reported previously against the same n-SYB peptide (6), and was found to detect n-SYB by Western blot analysis. The antiserum was purified as described (7) before its use for immunocytochemistry (1:10). Secondary antibodies included Alexa Fluor 568-conjugated anti-mouse or anti-rabbit IgG (1:200) (Invitrogen).

Immunocytochemical Analysis of Plasma Membrane SYNAPTOBREVIN. Genetic interaction studies of *Drosophila* TS paralytic mutants (8, 9) have suggested that NSF-mediated postfusion disassembly of plasma membrane SNARE complexes occurs at synapses as demonstrated directly in yeast (10). In an effort to address this issue directly at *Drosophila* synapses, we examined whether *comatose* (NSF) exhibits redistribution of the synaptic vesicle SNARE, SYNAPTOBREVIN (n-SYB) (11), to the plasma membrane as predicted for accumulation of plasma membrane *cis*-SNARE complexes. Immunocytochemical analysis was carried out using an antibody against the luminal (intravesicular) domain of synaptobrevin, which is accessible in unpermeabilized preparations only

when n-SYB is located in the plasma membrane. Analysis of unpermeabilized preparations used the same procedures as our conventional immunocytochemistry with the exception that Triton X-100 was omitted from all incubations. Control experiments confirmed that intracellular epitopes were not accessible in unpermeabilized preparations. The epitope recognized by anti-HRP is extracellular. In permeabilized preparations, the anti-n-SYB antibody produced strong labeling of synaptic vesicle clusters as expected for this abundant synaptic vesicle protein.

Substantial plasma membrane n-SYB was detected at resting or stimulated WT synapses (Fig. S7 *A–D*), consistent with previous work in other systems (12, 13). Also, in contrast to the active zone localization of t-SNAREs, plasma membrane n-SYB was widely distributed and appeared to be excluded from active zones. Under these conditions, comparison of stimulated WT and *comatose* (NSF) synapses was not expected to and did not demonstrate a clear difference in the distribution of plasma membrane n-SYB (Fig. S7). However, these studies have further defined the spatial relationship of v- and t-SNARE proteins in the presynaptic plasma membrane. Although it could not be confirmed that redistributed t-SNAREs are associated with plasma membrane n-SYB at *comatose* (NSF) synapses, biochemical studies demonstrating accumulation of plasma membrane ternary SNARE complexes (14) suggest this is the case.

1. Koenig JH, Kosaka T, Ikeda K (1989) The relationship between the number of synaptic vesicles and the amount of transmitter released. *J Neurosci* 9:1937–1942.
2. Kawasaki F, Mattiuz AM, Ordway RW (1998) Synaptic physiology and ultrastructure in *comatose* mutants define an *in vivo* role for NSF in neurotransmitter release. *J Neurosci* 18:10241–10249.
3. Rao SS, et al. (2001) Two distinct effects on neurotransmission in a temperature-sensitive SNAP-25 mutant. *EMBO J* 20:6761–6771.
4. Wagh DA, et al. (2006) Bruchpilot, a protein with homology to ELKS/CAST, is required for structural integrity and function of synaptic active zones in *Drosophila*. *Neuron* 49:833–844.
5. Sone M, et al. (2000) Synaptic development is controlled in the periactive zones of *Drosophila* synapses. *Development* 127:4157–4168.
6. van de Goor J, Ramaswami M, Kelly R (1995) Redistribution of synaptic vesicles and their proteins in temperature-sensitive *shibire* (ts1) mutant *Drosophila*. *Proc Natl Acad Sci USA* 92:5739–5743.
7. Zou B, Yan H, Kawasaki F, Ordway RW (2008) MAP1 structural organization in *Drosophila*: *In vivo* analysis of FUTSCH reveals heavy and light chain subunits generated by proteolytic processing at a conserved cleavage site. *Biochem J* 414:63–71.
8. Littleton JT, et al. (2001) SNARE-complex disassembly by NSF follows synaptic-vesicle fusion. *Proc Natl Acad Sci USA* 98:12233–12238.
9. Sanyal S, Tolar LA, Pallanck L, Krishnan KS (2001) Genetic interaction between shibire and comatose mutations in Drosophila suggest a role for snap-receptor complex assembly and disassembly for maintenance of synaptic vesicle cycling. *Neurosci Lett* 311:21–24.
10. Grote E, Carr CM, Novick PJ (2000) Ordering the final events in yeast exocytosis. *J Cell Biol* 151:439–451.
11. DiAntonio A, et al. (1993) Identification and characterization of *Drosophila* genes for synaptic vesicle proteins. *J Neurosci* 13:4924–4935.
12. Fernández-Alfonso T, Kwan R, Ryan TA (2006) Synaptic vesicles interchange their membrane proteins with a large surface reservoir during recycling. *Neuron* 51:179–186.
13. Taubenblatt P, Dedieu JC, Gulik-Krzywicki T, Morel N (1999) VAMP (synaptobrevin) is present in the plasma membrane of nerve terminals. *J Cell Sci* 112:3559–3567.
14. Tolar LA, Pallanck L (1998) NSF function in neurotransmitter release involves rearrangement of the SNARE complex downstream of synaptic vesicle docking. *J Neurosci* 18:10250–10256.
15. Wu Y, Kawasaki F, Ordway RW (2005) Properties of short-term synatic depression at larval neuromuscular synapses in wild-type and temperature-sensitive paralytic mutants of *Drosophila*. *J Neurophysiol* 93:2936–2405.

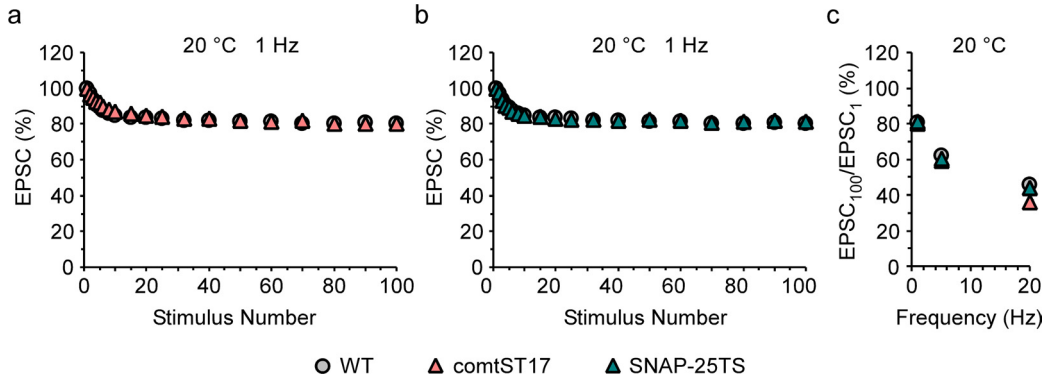

Fig. S1. At a permissive temperature of 20 °C, synaptic function in *comatose*^{ST17} (comtST17) and *SNAP-25*^{TS} closely resembles that of WT. Normalized peak EPSC amplitudes during a 1-Hz stimulation train (100 pulses) in *comatose* (NSF) (*a*) and *SNAP-25*^{TS} (*b*) are plotted as a function of stimulus number. (*c*) Similarity of short-term depression as a function of stimulation frequency at WT, *comatose* (NSF), and *SNAP-25*^{TS} mutant synapses at 20 °C. EPSC amplitudes in response to the 100th stimulus were normalized to the initial EPSC amplitudes ($EPSC_{100}/EPSC_0$), and plotted as a function of stimulation frequency ($n = 3–10$).

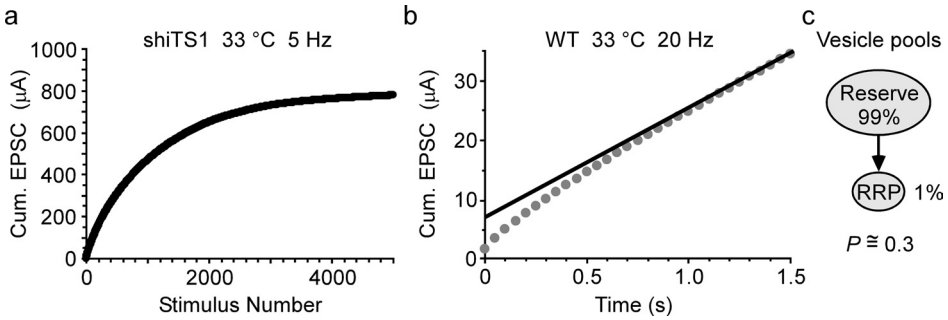

Fig. S2. Estimates of vesicle pool size and release probability at adult neuromuscular synapses. (*a*) The *shibire*^{TS1} mutant, in which synaptic vesicle endocytosis is thought to be blocked at restrictive temperatures, was used to estimate the total vesicle pool size (the total cumulative EPSC amplitude). Comparison of the total pool size (≈800 μA at 5,000 pulses) (*a*) with the release-ready pool size defined by the Y-intercept (6.8 μA) (*b*) indicates that ≈1% of vesicles reside in the release-ready pool as described for a wide range of model synapses (3). (*c*) Comparison of the estimated release-ready pool (6.8 μA) with the individual EPSC amplitude (2 μA; Fig. 1) yields an estimated release probability of ≈0.3.

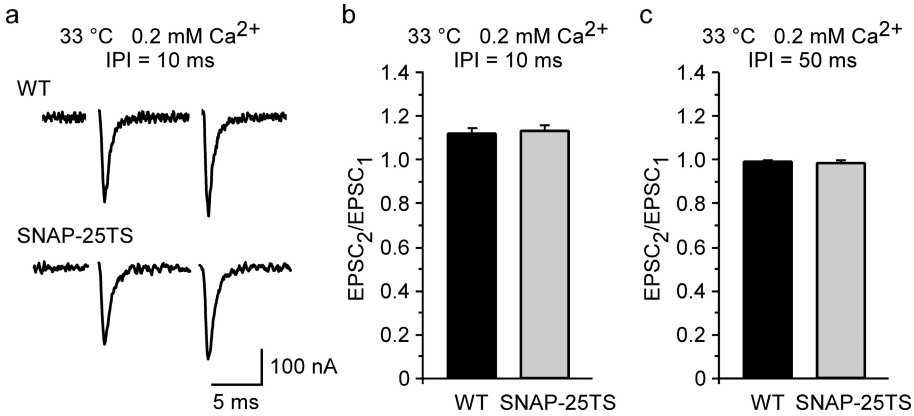

Fig. S3. WT paired-pulse facilitation in *SNAP-25^{TS}* under low release probability conditions suggests a use-dependent synaptic phenotype. (*a*) EPSCs elicited by PP stimulation of WT and *SNAP-25^{TS}* synapses in 0.2 mM extracellular calcium exhibit facilitation [interpulse interval (IPI) = 10 ms]. (*b*) PP ratios (R) ($EPSC_2/EPSC_1$) at an IPI of 10 ms indicate a similar degree of facilitation in WT (1.12 ± 0.02, $n = 4$) and *SNAP-25^{TS}* (1.13 ± 0.03, $n = 4$) at 33 °C. (*c*) PPRs at an IPI of 50 ms show no facilitation and are similar in WT (0.99 ± 0.01, $n = 3$) and *SNAP-25^{TS}* (0.98 ± 0.02, $n = 3$). In contrast, a clear PPD phenotype was observed in *SNAP-25^{TS}* at an IPI of 50 ms under normal physiological conditions [PPRs in WT and *SNAP-25^{TS}* were 82.6 ± 1.20 ($n = 4$) and 72.4 ± 1.38 ($n = 5$), respectively ($P = 0.001$)].

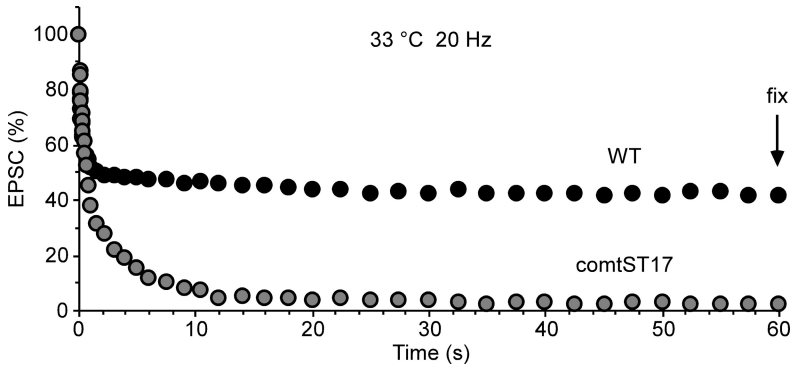

Fig. S4. The t-SNARE redistribution at *comatose* (NSF) DLM neuromuscular synapses. Peak EPSC amplitudes elicited by 20-Hz stimulation (1,200 pulses) of WT or *comatose*^{ST17} at 33 °C were normalized and plotted as a function of time. At the end of the stimulus train (arrow), preparations were fixed at 33 °C and processed for immunocytochemistry.

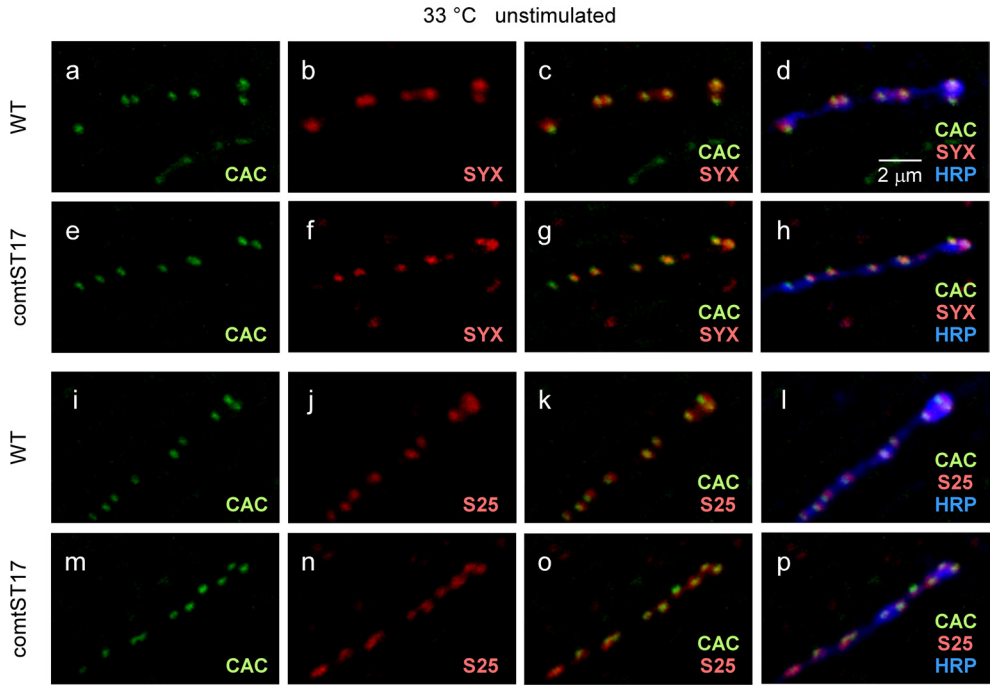

Fig. S5. The t-SNARE distribution at unstimulated WT and *comatose* (NSF) DLM neuromuscular synapses at the restrictive temperature of 33 °C. Confocal immunofluorescence imaging of endogenous SYNTAXIN (SYX) (*a–h*) and SNAP-25 (S25) (*i–p*). WT and *comatose* (NSF) preparations were maintained at 33 °C for 7 min without stimulation, fixed at 33 °C, and processed for immunocytochemistry. CAC-EGFP (CAC) and anti-HRP were used as active zone and neuronal plasma membrane markers, respectively. At unstimulated WT and *comatose* (NSF) synapses, both SYNTAXIN and SNAP-25 remained associated with active zone regions. All images represent maximum projections of two optical sections.

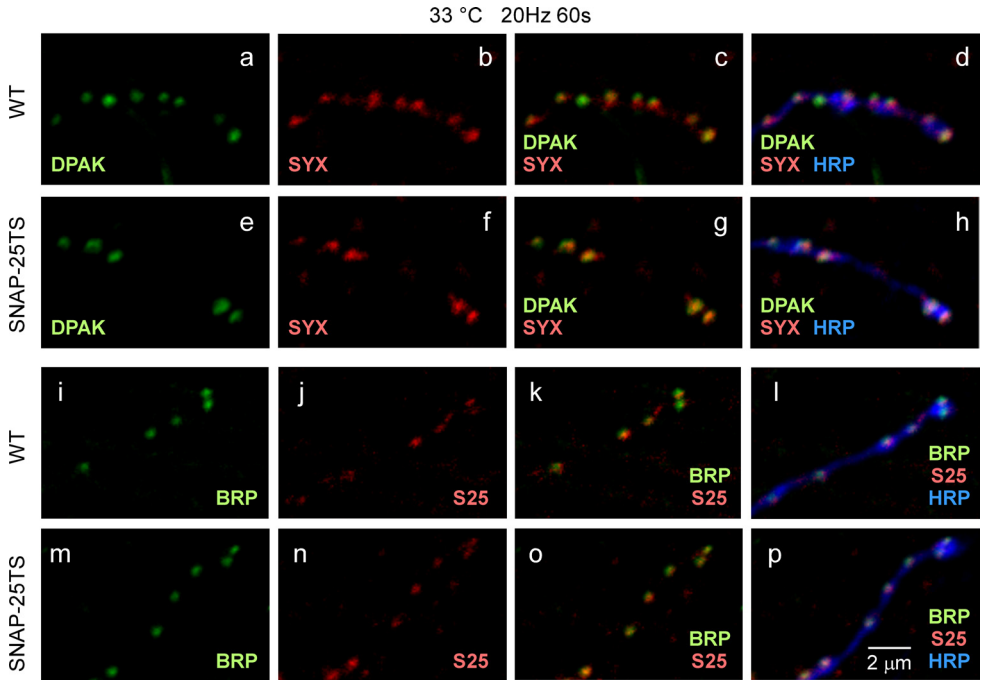

Fig. S6. The t-SNARE distribution at stimulated WT and *SNAP-25^{TS}* DLM neuromuscular synapses at the restrictive temperature of 33 °C. Confocal immunofluorescence imaging of endogenous SYNTAXIN (*a–h*) and SNAP-25 (S25) (*i–p*). WT and *SNAP-25^{TS}* synapses were subjected to 20-Hz stimulation (1,200 pulses) at 33 °C. At the end of the stimulus train, preparations were fixed at 33 °C and processed for immunocytochemistry. Anti-HRP was used as neuronal plasma membrane marker. Anti-DPAK (*Drosophila* p21-activated kinase) labeled postsynaptic densities apposing presynaptic active zones (*a–h*) and anti-BRP (BRUCHPILOT) was used as active zone marker (*i–p*). At both WT and *SNAP25^{TS}* synapses after 20-Hz stimulation at 33 °C, both SYNTAXIN and SNAP-25 remained associated with active zones. All images represent maximum projections of two optical sections.

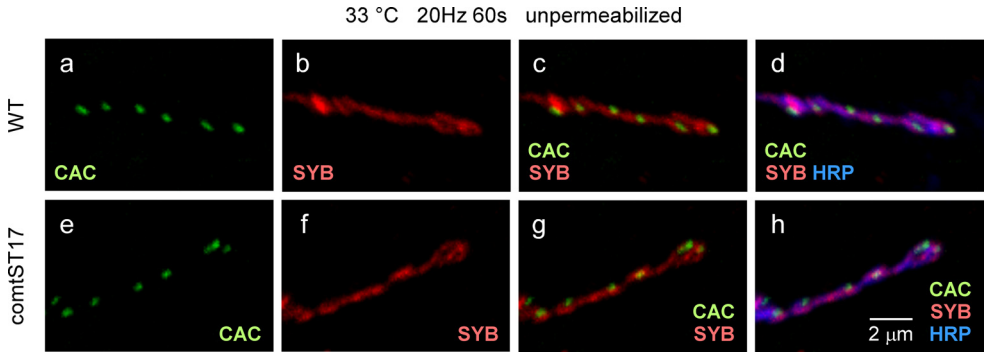

Fig. S7. The v-SNARE distribution in the plasma membrane of DLM neuromuscular synapses. Confocal immunofluorescence imaging of endogenous plasma membrane n-SYNAPTOBREVIN (SYB) in unpermeabilized preparations. WT and *comatose* (NSF) synapses were subjected to 20-Hz stimulation (1,200 pulses) at 33 °C. At the end of the stimulus train, preparations were fixed at 33 °C and processed for immunocytochemistry in the absence of detergent permeabilization. An antibody directed against the luminal (intravesicular) domain was used to label only n-SYNAPTOBREVIN located in the plasma membrane. At both WT and *comatose* (NSF) synapses, plasma membrane n-SYNAPTOBREVIN was broadly distributed and appeared to be excluded from active zones.

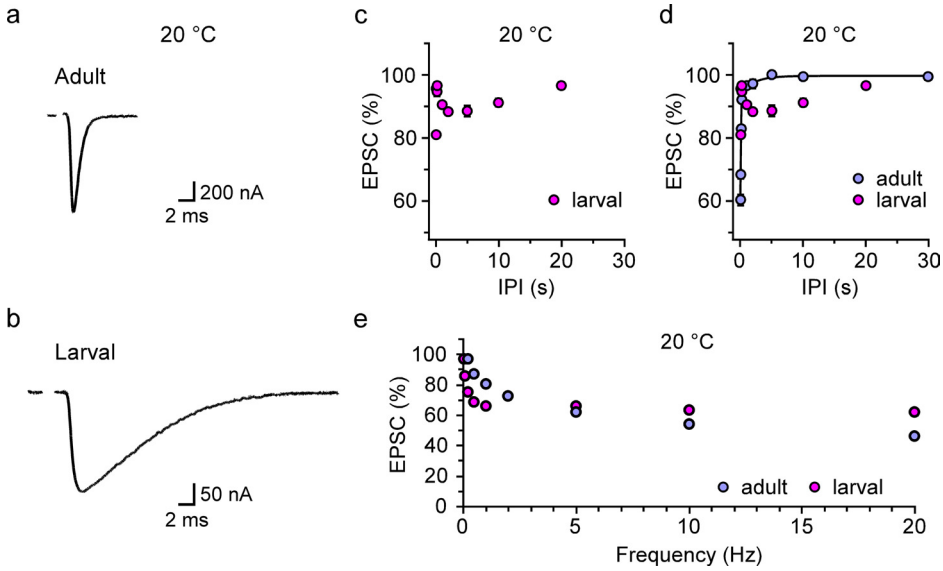

Fig. S8. Comparison of adult and larval synapses. The properties of short-term synaptic depression defined in our previous analysis of larval neuromuscular synapses (15) are compared with adult neuromuscular synapse properties reported here. (*a* and *b*) EPSC waveform at adult and larval neuromuscular synapses. (*c*) PPD at larval neuromuscular synapses exhibits a peak in the recovery time course at short IPIs followed by a very slow component of recovery consistent with low-frequency short-term depression (LF-STD) (15). (*d*) Comparison of PPD at larval versus adult neuromuscular synapses. (*e*) Frequency dependence of steady-state depression at larval versus adult neuromuscular synapses. Larval synapses exhibit marked depression at relatively low stimulation frequencies and are relatively insensitive to frequency over a moderate range (1–20 Hz).